

## Polarized site-selected fluorescence spectroscopy of isolated Photosystem I particles

Bas Gobets<sup>a</sup>, Herbert van Amerongen<sup>a</sup>, René Monshouwer<sup>a</sup>, Jochen Kruij<sup>b</sup>,  
Matthias Rögner<sup>b</sup>, Rienk van Grondelle<sup>a</sup>, Jan P. Dekker<sup>a,\*</sup>

<sup>a</sup> Department of Physics and Astronomy and Institute of Molecular Biological Sciences, Vrije Universiteit, De Boelelaan 1081, 1081 HV Amsterdam, The Netherlands

<sup>b</sup> Institute of Botany, University of Münster, Schloßgarten 3, D-48149 Münster, Germany

Received 27 January 1994

### Abstract

Polarized steady-state fluorescence spectra have been obtained from Photosystem I core complexes of the cyanobacterium *Synechocystis* PCC 6803 and from LHC-I containing Photosystem I (PS I-200) complexes of spinach by selective laser excitation at 4 K. Excitation above 702 nm in *Synechocystis* and 720 nm in PS I-200 results in highly polarized emission, suggesting that pigments absorbing at these and longer wavelengths are not able to transfer excitation energy at 4 K. In both systems the peak wavelength of the emission ( $\lambda_{em}$ ) depends strongly on the excitation wavelength ( $\lambda_{ex}$ ). This indicates that in both systems the long-wavelength bands responsible for the steady-state emission are inhomogeneously broadened. The width of the inhomogeneous distribution is estimated to be about 215  $cm^{-1}$  in *Synechocystis* and 400  $cm^{-1}$  in PS I-200. We conclude that the peaks of the total absorption spectra of the long-wavelength pigments of *Synechocystis* and PS I-200 are at 708 and 716 nm, respectively, and therefore designate these pigments as C-708 and C-716. The results further show that C-708 and C-716 are strongly homogeneously broadened, i.e. carry broad phonon side-bands. The width of these bands is estimated to be about 170 and 200  $cm^{-1}$  for C-708 and C-716, respectively. The Stokes' shifts appear to be large: about 200  $cm^{-1}$  (10 nm) for C-708 and about 325  $cm^{-1}$  (17 nm) for C-716. These values are much higher than usually observed for 'normal' antenna pigments, but are in the same order as found previously for a number of dimeric systems. Therefore, we propose that the long-wavelength pigments in Photosystem I are excitonically coupled dimers. Based on fitting with Gaussian bands the presence of one C-708 dimer per P700 is suggested in the core antenna of *Synechocystis*.

**Keywords:** Photosystem I; Spectroscopy; Polarized fluorescence; Site selection; (*Synechocystis*)

### 1. Introduction

The two main functions of the light-harvesting antenna pigments in photosynthetic systems are the absorption of light of different wavelengths and the efficient transfer of excitation energy to one of the photochemical reaction centers. Both functions are highly optimized in photosynthetic organisms: the antenna usually absorbs as much as possible of the available

light, and excitation energy transfer to the reaction center is generally highly efficient [1].

In Photosystem (PS) I of green plants, algae and cyanobacteria it has been shown that excitation energy transfer is indeed extremely rapid [2]. The most recent experiments suggest average single transfer times of about 180 fs [3] and overall trapping times in the tens of picoseconds time range [4–6]. According to Trissl [6,7] these processes in PS I are even more efficient than actually required, due to which the photosystem can afford a small number of antenna pigments absorbing at lower energy than the primary electron donor P700, thus increasing the absorption cross-section for red light (> 700 nm) and optimizing the balance between the two main functions. In addition, some of the

Abbreviations: CD, circular dichroism; Chl, chlorophyll; fwhm, full width at half maximum; LD, linear dichroism; LHC, light-harvesting complex; PS, Photosystem.

\* Corresponding author. Fax: +31 20 4447899.

long-wavelength pigments could help in guiding the excitations to P700 [4,8]. The long-wavelength pigments largely determine the steady-state emission properties at low temperatures. Such pigments in most of the PS I reaction center core complexes of green plants, algae and cyanobacteria give rise to emission bands peaking near 720 nm at 77K, while most of the peripheral chlorophyll *a/b* antenna complexes give rise to emission bands peaking near 735 nm [9].

Despite substantial interest in the role of long-wavelength pigments of PS I in excitation energy transfer and trapping, there is still considerable lack of knowledge about their molecular properties. The number of red pigments per complex, the exact absorption maxima, the extent of homogeneous and inhomogeneous broadening and the possibility of energy transfer between the red pigments are, for instance, not well known.

In a previous report, we analyzed a number of isolated PS I preparations (monomeric and trimeric core complexes from the cyanobacterium *Synechocystis* PCC 6803 and LHC-I containing PS I-200 complexes from spinach) by steady-state polarized light spectroscopy at 77 K [10] and linear and circular dichroism characteristics were established. It was concluded that the possibility of energy transfer between the various long-wavelength pigments was very low in the monomeric and trimeric particles from *Synechocystis*, but high in PS I-200, in which significant downhill energy transfer from the long-wavelength pigments of the core antenna to the peripheral antenna was proposed.

In this report, we extend this research by polarized site-selected fluorescence spectroscopy, provide new information on the spectroscopic properties of the long-wavelength pigments in the core and peripheral antenna of PS I, and propose that these pigments are arranged as excitonically coupled dimers of Chl *a*.

## 2. Materials and methods

Monomeric and trimeric PS I core particles (P700- $F_A/F_B$ ) from *Synechocystis* sp. PCC 6803 were prepared as described before by Rögner and co-workers [11,12]. Unlike the complexes studied in Ref. [10], the absorption profiles at long wavelengths were similar for the monomeric and trimeric complexes and the membranes studied in this contribution (see Section 3). For a possible explanation we suggested [10] that the amplitude of the long-wavelength spectral component in the monomers varies per batch and depends on the severeness of the detergent treatment during the isolation procedure. Obviously, the monomeric complexes analyzed in this contribution are more native. LHC-I containing PS I-200 particles from spinach were pre-

pared as described by Van der Lee et al. [10]. For the low-temperature measurements, the particles were diluted in 20 mM Mes-NaOH, 10 mM  $MgCl_2$ , 10 mM  $CaCl_2$ , 70% w/v glycerol and 0.05% dodecyl- $\beta$ ,D-maltoside (pH 6.5) and cooled to 4 K in a He-flow cryostat (Oxford).

Fluorescence spectra were obtained on a home-built fluorimeter and corrected for the sensitivity of the detection system as in Ref. [13]. Site-selection was performed as in [14], except that as light source for the site-selection excitation light a Ti-Sapphire laser was used (Coherent, model 890, spectral bandwidth  $\sim 2$   $cm^{-1}$ ). The laser was tuned between 693.5 and 733.5 nm at 1 nm intervals, using 4–20  $mW/cm^2$  energy. It was checked that no sample degradation took place during the measurements. Detection of the fluorescence was at right angle with respect to the excitation beam and was achieved with a double 1/8 m monochromator (Oriel) and a photomultiplier (S-20 photocathode, Thorn EMI 9658A). The spectral bandwidth for detection was 1.5 nm. The excitation light was vertically polarized (when sensitivity corrections were made horizontally polarized excitation was used as well) and a polarizer in the detection beam was either vertical or horizontal. The anisotropy of the emission is defined by  $r = (I_{\parallel} - I_{\perp}) / (I_{\parallel} + 2I_{\perp})$ , in which  $I_{\parallel}$  and  $I_{\perp}$  are the fluorescence intensities with vertical and horizontal detection beam polarizations, respectively. The site-selected spectra were recorded with  $A_{680} \sim 1$ . This high  $A$  was used to increase the fluorescence intensity. Self-absorption of the emitted light did not pose a serious problem, because the fluorescence appeared far away from the maximum of the absorption. Absorption spectra were measured on a Cary 219 spectrophotometer with 0.25 nm resolution.

## 3. Results

### 3.1. Photosystem I core complexes from *Synechocystis*

Cyanobacteria like *Synechocystis* contain reaction center core complexes of PS I, but lack peripheral Chl *a/b* containing antenna complexes. Isolated cyanobacterial cores, including those of *Synechocystis*, have been isolated as monomeric and/or as trimeric complexes [15,12]. There is increasing evidence that the trimeric association represents the in vivo organization of the cyanobacterial core under certain salt conditions [16–18], presumably in equilibrium with the monomer [18].

Fig. 1 shows Soret-excited emission spectra from monomeric PS I core complexes from *Synechocystis* sp. PCC 6803 between 4 K and 120 K. The spectra are characterized by a strongly temperature-dependent contribution peaking at about 720 nm (the exact peak maxima are 720.5 nm at 77 K and at 718.5 nm at 4 K)

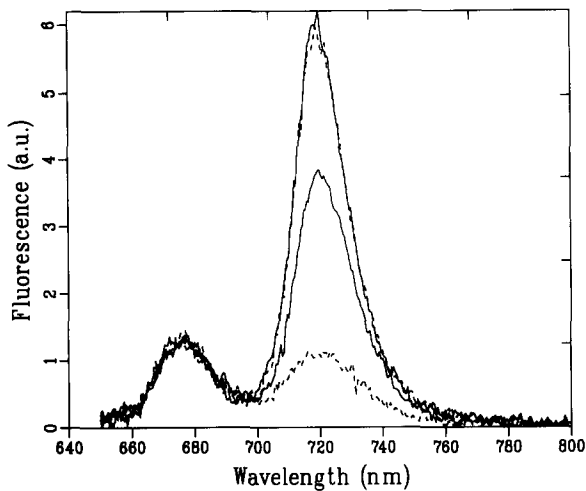


Fig. 1. Soret excited (437 nm) emission spectra of monomeric PS I complexes from *Synechocystis* PCC 6803 at 4 K (full line, upper curve), 40 K (dashed line, upper curve), 77 K (full line, lower curve) and 120 K (dashed line, lower curve). The spectra were recorded with  $A_{680} \sim 0.05$ .

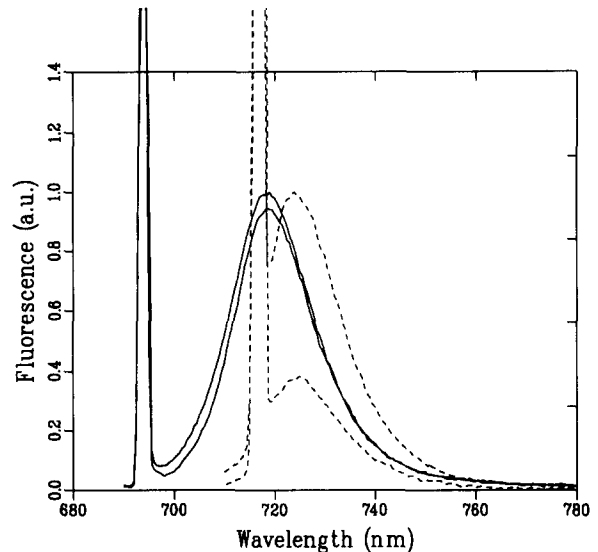


Fig. 2. Emission spectra at 4 K of monomeric PS I complexes from *Synechocystis* PCC 6803, laser-excited at 693.5 nm (full lines) and at 716.5 nm (dashed lines). The laser excitation light was vertically polarized, and a polarizer in the detection beam selected either for vertically polarized light (upper curves) or for horizontally polarized light (lower curves). The spectra were recorded with  $A_{680} \sim 1$  (see Section 2).

and a small temperature-independent contribution peaking at 675.5 nm. We attribute the latter contribution to uncoupled Chl absorbing at about 670 nm. The temperature-dependence of the 720 nm contribution is virtually identical to the dependence observed by Wittmershaus et al. for *Synechocystis* membranes [19].

The nature of the emission at 4 K was further analyzed by applying selective laser excitation in the red part of the Chl  $Q_{y(0-0)}$  absorption region. Fig. 2 shows a typical result of the vertically and horizontally polarized emission spectra of monomeric complexes upon vertical excitation at 693.5 nm (continuous lines) and 716.5 nm (dashed lines). The spectra consist of sharp, high peaks at the laser excitation wavelength and broad features around 720 nm that resemble the PS I emission peaks obtained by excitation in the Soret absorption region of the chlorophylls (Fig. 1). The contribution of uncoupled Chl is not observed with both excitation wavelengths, which is expected because the excitation wavelength is well above their absorption maximum [14]. The sharp features in Fig. 2 are largely due to elastic scattering of the laser excitation light. Also the contribution at the blue side of the scattering peak was found to originate from scattering, which was concluded from measurements on scattering samples without absorption at the wavelength of excitation.

It becomes immediately clear from Fig. 2 that the anisotropy of the emission depends strongly on the excitation wavelength. The vertically and horizontally detected emission spectra have about equal amplitudes upon 693.5 nm excitation, whereas they differ considerably upon 716.5 nm excitation. Fig. 3 shows the anisotropy spectra of the emission upon selective excitation at wavelengths from 693.5 nm to 705.5 nm. At all

excitation wavelengths at and above 705.5 nm the anisotropy is high ( $\sim 0.34$ ) and close to the theoretical maximum (0.4). This indicates that no depolarization due to energy transfer takes place at these wavelengths, although the possibility of energy transfer between pigments with almost perfectly aligned  $Q_y$  transitions cannot be ruled out. In Fig. 4a (open squares) the value of the anisotropy detected at 735 nm is plotted. It shows a steep rise from almost zero at 693.5 nm to about 0.34 above 705.5 nm and is almost identi-

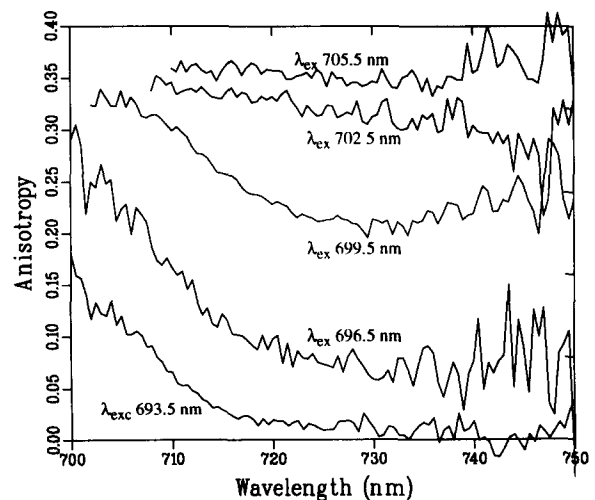


Fig. 3. Anisotropy spectra at 4 K of monomeric PS I complexes from *Synechocystis* PCC 6803, laser-excited (from bottom-to-top) at 693.5, 696.5, 699.5, 702.5 and 705.5 nm.

cal to the fluorescence polarization spectra at 77 K [10]. For excitation wavelengths between 693.5 and 705.5 nm the anisotropy of the emission depends on the detection wavelength; close to the scattering peak at the blue side of the emission band the anisotropy increases to some extent (Fig. 3). This is not due to a contribution of polarized scattered light (anisotropy 1.0), because the region of increased anisotropy extends more to the red than the scattered light and because it is not observed upon excitation above 705.5 nm.

Another feature of the site-selected emission spectra of Fig. 2 is that the peak-wavelength of the emission depends on the excitation wavelength. The values of the emission maxima are plotted in Fig. 4a (closed circles) as a function of excitation wavelength. Striking is the fact that upon redshifting the wavelength of excitation the emission maximum first blueshifts to about 717 nm upon excitation at 702 nm, and then redshifts with a slope of about 0.6. Fig. 5 compares the shapes of the emission spectra obtained upon relatively blue (693.5 nm) and relatively red excitation (712.5 nm). The width and shape on the red side of the emission spectra are very similar, whereas the width on the blue side decreases upon far red excitation. The same phenomenon was also observed in the antenna of *Rhodospseudomonas viridis* (R. Monshouwer et al., unpublished observations).

Fig. 4b and c show that site-selected fluorescence measurements on trimeric particles and thylakoid membranes from *Synechocystis* sp. PCC 6803 yield basically the same results as obtained for monomeric particles. This shows that the long-wavelength pigments that are responsible for the steady-state emission at 4 K are basically unperturbed during the isolation procedure. This also indicates that in the trimeric particles there is no excitation energy transfer among the long-wavelength pigments at 4 K (which confirms conclusions in Ref. [10] at 77 K), because otherwise the anisotropy and peak wavelength of emission would show a dependence on excitation wavelength different from that observed in the monomers.

### 3.2. PS I-200 complexes from spinach

Polarized site-selected fluorescence experiments were also performed on PS I-200 complexes from spinach. These complexes consist of a monomeric PS I core surrounded by about 8 Chl *a/b* containing LHC-I proteins [20]. The latter proteins contain long-wavelength pigments that are responsible for steady-state fluorescence peaking at about 735 nm [9]. These pigments absorb and fluoresce more to the red than the long-wavelength pigments of the core antenna of PS I. Van der Lee et al. [10] suggested that excitations are effectively transferred from the long-wavelength pig-

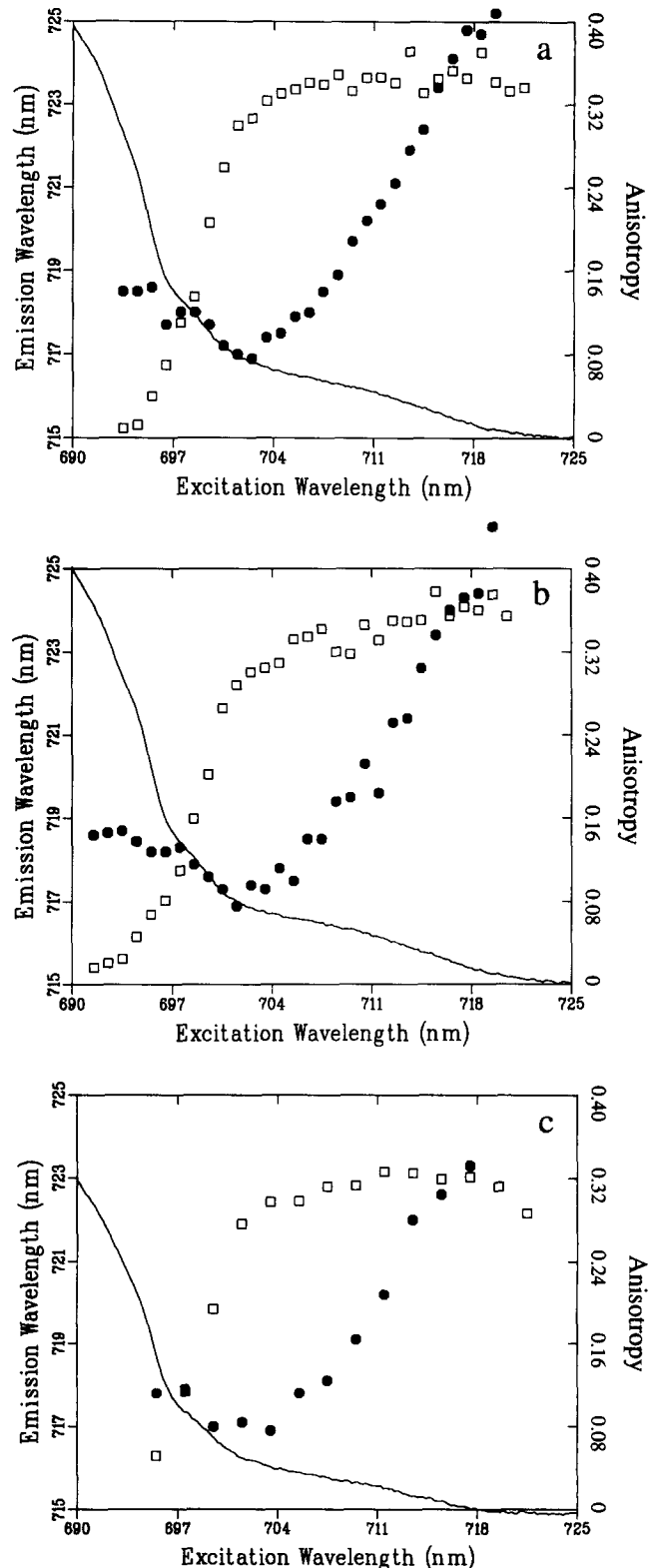


Fig. 4. (A) Emission and absorption characteristics of monomeric PS I complexes from *Synechocystis* PCC 6803 at 4 K. Closed circles: wavelength of the emission maximum ( $\lambda_{em}$ ) as a function of excitation wavelength ( $\lambda_{ex}$ ). Open squares: value of the anisotropy of the emission detected at 735 nm. Line: 4 K absorption spectrum. (B) As A, but of trimeric PS I complexes from *Synechocystis* PCC 6803 at 4 K. (C) As A, but of thylakoid membranes from *Synechocystis* PCC 6803 at 4 K.

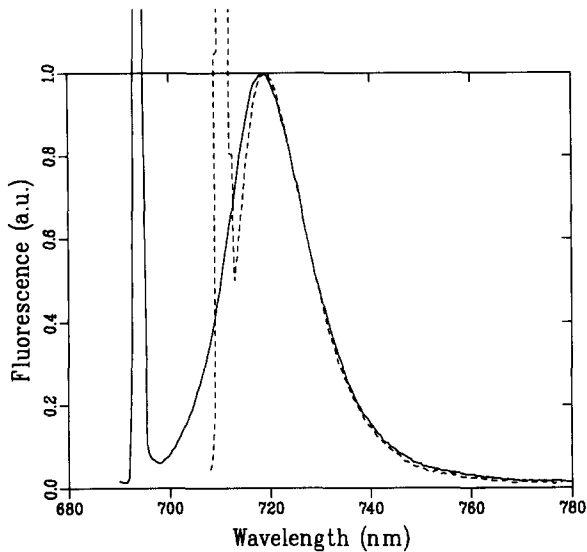


Fig. 5. Comparison of the spectral shape of emission spectra of monomeric PS I complexes from *Synechocystis* PCC 6803 at 4 K excited at 693.5 nm (full line) and 712.5 nm (dashed line, blue-shifted by 2 nm). The spectra were normalized at the peak of the emission at 718.5 nm.

ments of the core antenna to the long-wavelength pigments of the peripheral antenna at low temperatures.

Fig. 6 shows a typical result of polarized site-selected fluorescence experiments of PS I-200. Again, pronounced scattering peaks are observed around the excitation wavelength, as well as excitation-wavelength dependent anisotropies and peak wavelengths of the

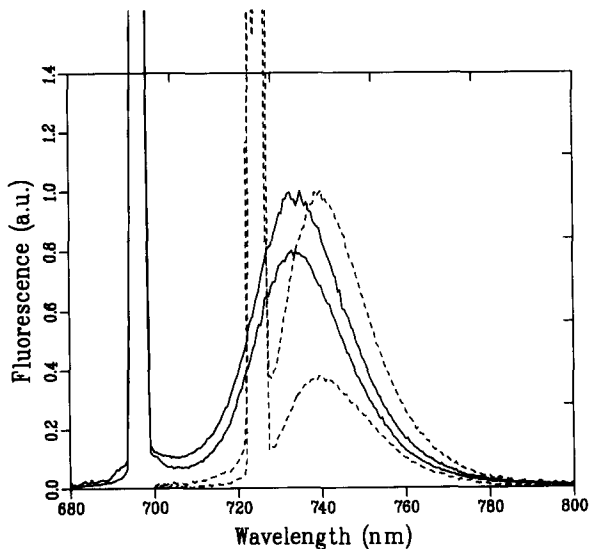


Fig. 6. Emission spectra at 4 K of PS I-200 complexes from spinach, laser-excited at 695.5 nm (full lines) and at 723.5 nm (dashed lines). The laser excitation light was vertically polarized, and a polarizer in the detection beam selected either for vertically polarized light (upper curves) or for horizontally polarized light (lower curves). The spectra were recorded with  $A_{680} \sim 1$  (see Section 2).

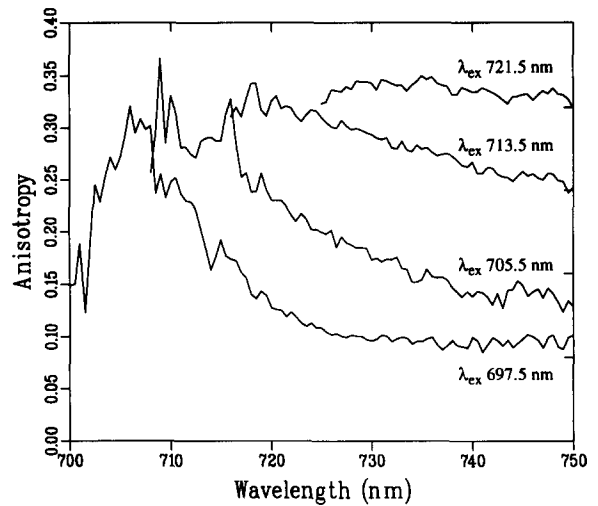


Fig. 7. Anisotropy spectra at 4 K of PS I-200 complexes from spinach, laser-excited (from bottom-to-top) at 697.5, 705.5, 713.5 and 721.5 nm.

emission. The anisotropy spectra of the emission for a number of applied excitation wavelengths are shown in Fig. 7. For excitation wavelengths from 695.5 to 713.5 nm it shows a region of increased anisotropy close to the excitation wavelength, similar to excitation wavelengths below 705.5 nm in the PS I core particles from *Synechocystis*. As the excitation wavelength is shifted from the blue to the red side of this region, the red tail of the anisotropy rises until the anisotropy spectra are constant over the entire emission band. The flat, high anisotropy occurs with excitation wavelengths at and above 721.5 nm (see also Fig. 8, open squares). The peak wavelength of the emission is constant at excita-

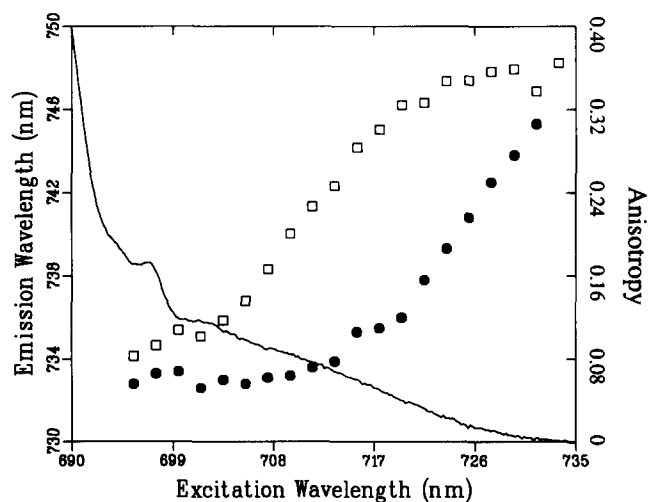


Fig. 8. Emission and absorption characteristics of PS I-200 complexes from spinach at 4 K. Closed circles: wavelength of the emission maximum ( $\lambda_{em}$  as a function of excitation wavelength ( $\lambda_{ex}$ ). Open squares: value of the anisotropy of the emission detected at 750 nm. Line: 4 K absorption spectrum.

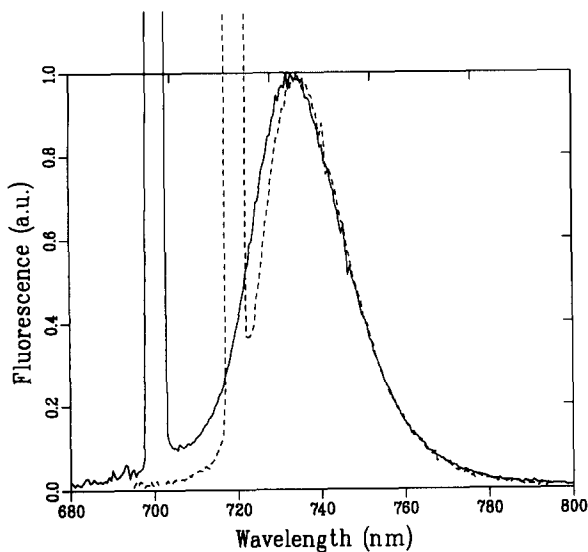


Fig. 9. Comparison of the spectral shape of emission spectra of PS I-200 complexes from spinach at 4 K excited at 699.5 nm (full line) and 723.5 nm (dashed line, blueshifted by 5 nm). The spectra were normalized at the peak of the emission at 733.5 nm.

tion wavelengths below 715 nm (Fig. 8, closed circles). Above 719 nm it starts to rise almost linearly upon redshifting the excitation with a slope of about 0.77. This slope is steeper than the slope observed in the PS I particles of *Synechocystis*, and a dip as in the corresponding experiments on *Synechocystis* (Fig. 4a–c, closed circles) is not observed. Fig. 9 compares the shapes of the emission spectra obtained upon relatively blue (699.5 nm) and relatively red excitation (723.5 nm). As in *Synechocystis*, the width and shape on the red side of the emission spectra are the same, whereas the width on the blue side decreases upon far red excitation.

#### 4. Discussion

The polarized site-selected emission experiments of PS I reaction center core and peripheral antenna complexes presented in this contribution show that anisotropy and peak wavelength of the emission depend on the excitation wavelength. Polarized site-selected emission experiments have also been performed on isolated LH1 antenna complexes from *Rhodobacter sphaeroides* [21], the B820 subunit of the LH1 antenna complex of *Rhodospirillum rubrum* [22], Chl *a* in detergent [14] and the isolated PS II reaction center complex [23], and results of these experiments have been explained in terms of downhill energy transfer among a specific cluster of pigments and homogeneous and inhomogeneous broadening of spectral bands.

#### 4.1. Inhomogeneous broadening

In general, spectral lines can be inhomogeneously and homogeneously broadened [24–26]. Inhomogeneous broadening of the absorption bands ( $\Gamma_i$ ) reflects variations in the energies of the electronic transitions of the pigments. These variations arise from slightly different conformations of the protein environment of the pigment. The various conformations will be frozen at very low temperatures, due to which pigments in those conformations can selectively be excited by steady-state laser light. Homogeneous broadening ( $\Gamma_h$ ) is usually defined as broadening of the zero-phonon transition. Another form of broadening, which also may be regarded as a form of homogeneous broadening, stems from electron-phonon coupling, which leads to asymmetric broadening towards the high-energy side of the absorption band, reflected by a phonon side-band. The phonon side-band actually carries a significant part of the oscillator strength of the transition; it will also appear in the fluorescence spectrum but then on the low-energy side of the zero-phonon line. In the remaining part of this paper we will refer to  $\Gamma_h$  as the width of the phonon side-wing, since this wing is much broader than the zero-phonon line.

The site-selected emission spectra of the PS I core and peripheral antenna complexes presented in this contribution show that the optical transitions of the long-wavelength pigments responsible for the steady-state emission are considerably inhomogeneously broadened, since the shape and position of the emission spectrum depend on the excitation wavelength (see Appendix). We just note here that homogeneous broadening is also very significant for the description of the spectral properties of the long-wavelength pigments (see below).

The concept of inhomogeneous broadening has consequences for the shape of the PS I core emission spectra at intermediate temperatures (e.g., 77 K). At these temperatures there is slow uphill energy transfer from the long-wavelength pigments to the primary electron donor P700, which forms a very efficient energy trap. The uphill transfer will be more efficient for long-wavelength pigments absorbing at the blue side of the inhomogeneous distribution than for those at the red side, due to which the red part will contribute more to the fluorescence. The spectra presented in Fig. 1 show that indeed the emission red-shifts upon raising the temperature from 4 K to 77 K, and therefore give further support to the inhomogeneous broadening of the long-wavelength pigments of PS I. This also shows that one has to be careful about assigning specific emission bands to specific pigments, because the emission spectrum may preferentially arise from a low-energy part of the inhomogeneous distribution.

#### 4.2. Energy transfer in the PS I antenna from *Synechocystis*

The anisotropy data presented in Ref. [10] and in Fig. 4 of this contribution suggest that the long-wavelength pigments in the core antenna of *Synechocystis* are either not connected by energy transfer or are connected but with almost parallel  $Q_y$  transition dipoles. However, the fact that anisotropy and peak wavelength of the emission start to rise and decrease, respectively, at the same excitation wavelength ( $\sim 695$  nm) rules out the option that parallel long-wavelength pigments are connected by energy transfer at 4 K. If two or more 'red' pigments would be coupled, the probability of energy transfer from a pigment on the blue side of the inhomogeneous distribution to another would be high, due to which the probability of emission at the blue side of the distribution would be low and the peak wavelength of emission would start to shift at a considerably longer excitation wavelength than the anisotropy (see also Ref. [21]).

The low anisotropy values of the emission obtained upon excitation at and below 695.5 nm are due to energy transfer from pigments which absorb below this wavelength and transfer their excitation energy to the long-wavelength pigments. Similarly, the high anisotropy values obtained upon excitation above 702 nm indicate the absence of energy transfer. Since just above 702 nm P700 should have significant absorption, it also indicates that there is no energy transfer from P700 to the long-wavelength pigments at 4 K, suggesting that P700 forms a perfect energy trap. At intermediate wavelengths a mixture of different types of pigments is excited. The resulting emission spectra revealed a relatively high anisotropy at the blue side of the emission band and a much lower anisotropy at the red side (Fig. 3). The high anisotropy at the blue side may arise from pigments which form local energy traps and transfer the energy relatively slowly (in 10–20 ps – see Ref. [1]) to P700 or to the long-wavelength antenna pigments.

#### 4.3. The homogeneous bandwidth of the long-wavelength pigments in *Synechocystis*

The plot of the peak wavelength of emission versus excitation wavelength (Fig. 4) also gives information about the relative width of the homogeneous lineshape of the long-wavelength pigments. From the anisotropy measurements it can be deduced that for excitation wavelengths above 702 nm the emission almost exclusively arises from directly excited long-wavelength pigments. The peak wavelength of the emission shifts from about 717 nm for 702 nm excitation to 725 nm for 719 nm excitation. It is remarkable that even at the latter wavelength at the far red end of the absorption

spectrum the gap between excitation and peak of emission wavelength is rather high (about 6 nm, or  $115 \text{ cm}^{-1}$ ). Since at this far-red excitation wavelength the pigments will be excited in their zero-phonon lines or in the red part of the phonon wing, a large proportion of this gap represents the energetic separation between the zero-phonon line and the peak of the corresponding phonon wing. Also the spectrum obtained upon far-red excitation has a quite considerable width (see, for instance, the 716.5 nm excited spectra in Fig. 2, which are characterized by a fwhm of about 16 nm or  $310 \text{ cm}^{-1}$ ).

Excitation at 708 nm yielded an emission maximum at 718.5 nm. The same maximum is observed upon non-selective excitation, which suggests that the peak position of the complete absorption band of all long-wavelength pigments is near 708 nm (see Appendix:  $\lambda_{\text{em}} = \lambda_{0,\text{em}}$  at 718.5 nm, due to which  $\lambda_0 = \lambda_{\text{ex}} = 708$  nm). We will therefore designate from now on the long-wavelength pigments of *Synechocystis* as C-708.

From the slope of the  $\lambda_{\text{em}}$  vs.  $\lambda_{\text{ex}}$  plot estimates for the homogeneous ( $\Gamma_h$ ) and inhomogeneous ( $\Gamma_i$ ) bandwidths can be obtained (see Appendix). The slope is not very large ( $s = 0.6$ ) and suggests  $\Gamma_h/\Gamma_i \sim 0.8$ . This means that C-708 is characterized by a quite considerable homogeneous bandwidth. From the Gaussian fit of Fig. 10 (discussed in detail below) a value of  $\sim 270 \text{ cm}^{-1}$  is estimated for the total fwhm of C-708 in absorption. Assuming Gaussian profiles for homogeneous and inhomogeneous broadening, this leads to values of  $\sim 170$  and  $215 \text{ cm}^{-1}$  for  $\Gamma_h$  and  $\Gamma_i$ , respectively. The energetic separation between the peak wavelengths of absorption and emission is about 10 nm (or  $200 \text{ cm}^{-1}$ ) for the total long-wavelength band, which largely represents the energetic separation between peak wavelengths of the phonon side bands in absorption and emission, i.e. the Stokes' shift  $\delta$ . The difference in shape of the emission spectra upon relatively blue and red excitation (Fig. 5) is attributed to the preferential excitation in the blue and red parts of the phonon wing, respectively.

The Stokes' shift of C-708 appears much larger than of isolated Chl *a* ( $\sim 80 \text{ cm}^{-1}$  – Ref. [14]). In principle, this large value could be due to specific interactions between the protein environment (e.g., charged amino acids) and monomeric Chl *a*. However, we are not aware of any documented precedents. Alternatively, the large Stokes' shift of C-708 may be caused by strong pigment–pigment interactions. An increased Stokes' shift was observed in the B820 subunit of the LH1 antenna of *Rhodospirillum rubrum* (about  $120 \text{ cm}^{-1}$  – Ref. [27]) and attributed to the dimeric nature of the BChls. Also for the primary electron donor of the reaction center of purple bacteria a large separation between zero-phonon line and peak wavelength of the phonon side band ( $\sim 120 \text{ cm}^{-1}$ ) was observed [25],

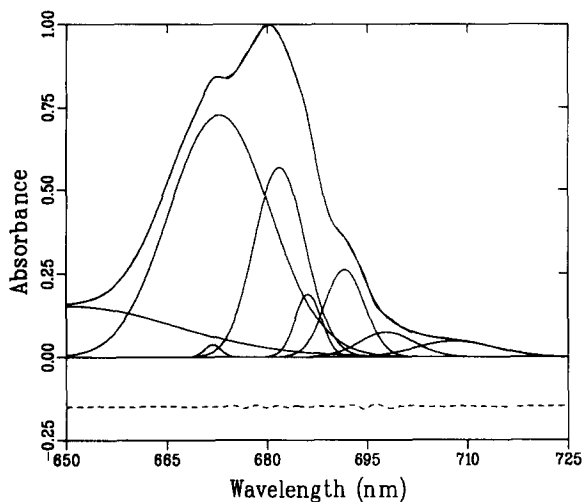


Fig. 10. Fit with Gaussian bands of the absorption spectrum between 650 and 725 nm of monomeric PS I complexes from *Synechocystis* PCC 6803 at 4 K. The dashed line represents the difference between absorption spectrum and fit, and is plotted with an offset of  $-0.15$ . Constraints: 8 Gaussians, each characterized by a certain peak wavelength ( $\lambda$ ), fwhm and amplitude ( $a$ ); all parameters were free fitting parameters. Result: band 1 (C-708):  $\lambda = 708.1$  nm, fwhm = 13.5 nm,  $a = 0.049$ ; band 2 (P700):  $\lambda = 697.9$  nm, fwhm = 9.5 nm,  $a = 0.076$ ; band 3:  $\lambda = 691.6$  nm, fwhm = 7.0 nm,  $a = 0.262$ ; band 4:  $\lambda = 686.1$  nm, fwhm = 4.6 nm,  $a = 0.190$ ; band 5:  $\lambda = 681.9$  nm, fwhm = 9.0 nm,  $a = 0.567$ ; band 6:  $\lambda = 672.8$  nm, fwhm = 17.7 nm,  $a = 0.812$ ; band 7:  $\lambda = 671.8$  nm, fwhm = 2.9 nm,  $a = 0.007$ ; band 8:  $\lambda = 650.6$  nm, fwhm = 36 nm,  $a = 0.154$ . The last band approximates a collection of vibrational bands of all spectral bands and is not included in the estimation of the oscillator strength in bands 1 and 2.

which predicts a Stokes' shift of about  $240 \text{ cm}^{-1}$ . Based on these results we propose that pigment–pigment interactions rather than pigment–protein interactions cause the large Stokes' shift of C-708 and that C-708 is a dimer of (excitonically coupled) Chl *a* molecules (see also below). The CD is less than that of P700 [10], which suggests that the electronic transition dipole moments of the individual molecules are more in one plane than those of P700. The transition dipole moment of the major exciton component of C-708 was reported to make an angle between  $17^\circ$  and  $28^\circ$  with the plane of the particle [10].

#### 4.4. The number of long-wavelength pigments in *Synechocystis*

In our earlier report [10] we mentioned that it was not possible to estimate the number of long-wavelength pigments per reaction center by fitting the absorption spectra with Gaussian bands. Several good fits could be obtained in which peak wavelength and amplitude of the long-wavelength pigments varied quite considerably. The more accurate estimation of the peak wavelength of C-708 in this contribution permits a better estimation of the oscillator strength of C-708. Fig. 10

shows a fit with Gaussian bands of the 4 K absorbance spectrum of monomeric complexes. The result is a 13.5 nm broad Gaussian with an oscillator strength of 1.85 per 65 Chls, suggesting one C-708 dimer per monomeric reaction center complex. The intensity of the P700 band at 698 nm was 2.05 per 65 Chls, in agreement with its dimeric nature. We do not wish to attribute much significance to the remaining part of the fit. The fit is consistent, however, with the wavelength dependent behavior of the anisotropy. Below 695 nm C-708 has no absorption. Therefore, upon excitation below 695 nm almost all fluorescence arises after excitation energy transfer. On the other hand, the 'blue' antenna pigments do not absorb above 701 nm and excitation above 701 nm leads to highly polarized fluorescence from directly excited pigments, in agreement with the results presented in Fig. 4. The data suggest that the PS I core antenna does not contain a separate pool of antenna pigments that absorbs between C-708 and the pool absorbing at 693 nm, and that C-708 in *Synechocystis* may be regarded as a  $N = 1$  system.

#### 4.5. Comparison with results from spectral hole-burning

It is worthwhile to compare our site-selected fluorescence data on PS I core particles with the hole-burning data by Small and co-workers [28]. These authors analyzed PS I core particles from spinach, which showed an absorption maximum at considerably shorter wavelength than our particles ( $\sim 670$  nm vs. 679 nm), but nevertheless are characterized by rather similar absorption profiles in the far red absorption region (compare, e.g., Fig. 2 from Ref. [28] with Fig. 4 from this contribution). The hole-burning profiles were analyzed in absorption, which means that (depending on the burning efficiencies) P700 and C-708 may both contribute to the spectra and that the presented spectral parameters could arise from a mixture of both species. However, the presence of long-wavelength antenna pigments was not considered in Ref. [28].

The hole-burning profiles obtained after irradiation at 702.6, 706.3 and 715.0 nm could reasonably well be described by a Huang-Rhys factor  $S$  of 4–6 and a mean phonon frequency  $\omega_m$  of  $35\text{--}50 \text{ cm}^{-1}$  [28]. Because according to our fits (Fig. 10) P700 will primarily be excited at 702.6 nm and C-708 at 715 nm, we conclude that the spectral properties of both species do not differ very much. This suggests that the broad homogeneous linewidth of C-708 observed in the present study is mainly caused by a large value of  $S$ , i.e., by a considerable reorganization of C-708 in the excited state.

The product  $S\omega_m$  approximately represents the energetic separation between the zero-phonon line and the peak of the phonon side-band [25]. This product was estimated by Gillie et al. [28] to be  $\sim 200 \text{ cm}^{-1}$ ,

which is about twice as large as estimated from our site-selected fluorescence data. We do not have an appropriate explanation for this discrepancy. Nevertheless, both values are much larger than the value of  $S\omega_m \sim 20 \text{ cm}^{-1}$  obtained after burning in the 'normal' antenna at 680.5 nm [28]. This emphasizes the different nature of the long-wavelength antenna pigments as opposed to normal antenna pigments.

#### 4.6. Long-wavelength antenna pigments in PS I-200 from spinach

The situation in the core/peripheral antenna of PS I-200 is more complex than in the core antenna of *Synechocystis*. There are several pools of long-wavelength antenna pigments, and because the anisotropy starts to rise at a considerably longer wavelength than in the core antenna of *Synechocystis* and in isolated LHC-I [29], it is clear that at least some of these pools are connected by energy transfer. Excitation wavelengths longer than about 720 nm have to be applied in order to minimize the energy transfer.

The non-selectively excited steady-state emission spectrum is characterized by a broader bandwidth (fwhm  $\sim 470 \text{ cm}^{-1}$  vs.  $\sim 340 \text{ cm}^{-1}$  for *Synechocystis*). Because the slope of the  $\lambda_{em}$  vs.  $\lambda_{ex}$  plot is steeper ( $\sim 0.77$  in PS I-200 vs.  $\sim 0.6$  in *Synechocystis*) we suggest that an increase of the inhomogeneous bandwidth is primarily responsible for the increased emission bandwidth of the red-most pool of long-wavelength pigments in PS I-200. According to calculations as in the Appendix, we estimate  $\Gamma_h/\Gamma_1 \sim 0.55$ . With a somewhat higher value for  $\Gamma_h$  as in *Synechocystis* ( $\sim 200 \text{ cm}^{-1}$ ) and a  $1/0.55$  higher value for  $\Gamma_1$  ( $\sim 360 \text{ cm}^{-1}$ ), the total bandwidth in absorption will be  $\sim 400 \text{ cm}^{-1}$ , which seems a reasonable value.

The energetic separation between the zero-phonon line and the peak of the phonon wing (i.e., the value of  $S\omega_m$ ) should be relatively large in PS I-200, since excitation at the far red end of the absorption spectrum (732 nm) still yielded a shift of 13 nm ( $240 \text{ cm}^{-1}$ ), which is about twice as large as in the core antenna of *Synechocystis*. Thus, the shape of the emission spectra upon far red excitation differs considerably for the two analyzed systems: the value of  $S\omega_m/\Gamma_h$  is about 0.57 in *Synechocystis* and 1.0 in PS I-200. Because the value of  $S\omega_m$  is even larger in PS I-200 than in *Synechocystis*, we propose, in line with the discussions described above for *Synechocystis*, that pigment–pigment interactions also determine the spectroscopic properties of the red-most long-wavelength pigments in PS I-200.

The data also permit an estimation of the peak wavelength of the total absorption band of the long-wavelength pigments. Substituting values from the  $\lambda_{em}$  vs.  $\lambda_{ex}$  plot (for the region  $\lambda_{ex} > 720 \text{ nm}$  – see Fig. 8) into Eq. (A-8) yields  $\lambda_0 = 716 \text{ nm}$ . This value is some-

what less accurate than that of C-708, because it is uncertain in which extent the long wavelength pigments are connected by energy transfer. Introduction of energy transfer would shift the peak wavelength of the long-wavelength pigments to shorter wavelengths [21]. A Stokes' shift  $\delta$  of 17 nm, however, seems reasonable in view of the parameters described above. Therefore, we propose to denote the long-wavelength pigments in the peripheral antenna of PS I as C-716.

#### Acknowledgements

This research was supported in part by the Netherlands Foundations for Chemical Research (SON) and for Biophysics (SvB), financed by the Netherlands Organization for Scientific Research (NWO). J.P.D. was supported by a fellowship from the Royal Academy of Arts and Sciences (KNAW). J.K. and M.R. were supported by a grant from the Deutsche Forschungsgesellschaft (DFG).

#### Appendix

In this appendix the fluorescence behavior of a pool of non-transferring pigments upon site selected excitation is described. The position of the fluorescence maximum  $\lambda_{em}$  for excitation at a particular wavelength  $\lambda_{ex}$  depends on the relative contributions of homogeneous and inhomogeneous broadening to the absorption spectrum. In order to illustrate this we first consider two extreme cases:

- (1) The homogeneous broadening is negligible with respect to the inhomogeneous broadening. This is for instance the case when the absorption spectrum is solely determined by the zero-phonon line and the phonon sideband is absent. In that case both absorption and emission occur through the same zero-phonon transition and  $\lambda_{em} = \lambda_{ex}$ . This leads to a maximum value for the slope  $s$  defined as  $d(\lambda_{em})/d(\lambda_{ex})$ , namely  $s = 1$ ;
- (2) The inhomogeneous broadening is negligible with respect to the homogeneous broadening. In that case  $\lambda_{em}$  does not depend on  $\lambda_{ex}$  and  $s = 0$ . For pigments in a protein environment both types of broadening are significant and this leads to values of  $s$  between 0 and 1.

We consider now the case of individual pigments which do not transfer energy to each other. All pigments are assumed to have identically shaped absorption and emission spectra and the difference  $\delta$  between the absorption and emission maxima (Stokes' shift) is also assumed to be identical. In all cases a wavelength scale is used. A frequency (energy) scale would be more appropriate but is not necessary at the

current level of approximation. The maxima of the absorption spectra of individual pigments are distributed according to a distribution function  $SDF(\lambda)$ , which is usually taken to be Gaussian [30]:

$$SDF(\lambda) = \frac{1}{\sqrt{\pi} \sigma_i} e^{-(\lambda - \lambda_0)^2 / \sigma_i^2} \quad (A-1)$$

Here  $\lambda_0$  denotes the center of the distribution and  $\sigma_i$  is proportional to the inhomogeneous width  $\Gamma_i$  (fwhm) of the distribution according to  $\Gamma_i = 1.67\sigma_i$ . At first, the zero-phonon line will be omitted. Its effect will be discussed later. Therefore, the absorption spectrum is fully determined by the phonon sideband. Its shape is chosen to be Gaussian (see also below), since this allows an easy mathematical treatment. For a single chromophore with its absorption maximum at  $\lambda$ , the absorption at a particular wavelength of excitation  $\lambda_{ex}$  is given by:

$$\epsilon_\lambda(\lambda_{ex}) = \frac{1}{\sqrt{\pi} \sigma_h} e^{-(\lambda - \lambda_{ex})^2 / \sigma_h^2} \quad (A-2)$$

$\sigma_h$  is proportional to the width of the homogeneous broadening  $\Gamma_h$  (fwhm) according to  $\Gamma_h = 1.67\sigma_h$ . Note that the maximum of the total absorption spectrum is at  $\lambda_0$ . The maximum of the total fluorescence spectrum  $\lambda_{0,em}$  (which can be obtained upon non-selective excitation, e.g. in the Soret region) is then at  $\lambda_{0,em} = \lambda_0 + \delta$ .

The number of pigments  $N(\lambda)$  with an absorption maximum at  $\lambda$ , excited by excitation light with wavelength  $\lambda_{ex}$ , is proportional to  $P(\lambda)$  which is defined as

$$P(\lambda) = SDF(\lambda) \epsilon_\lambda(\lambda_{ex}) \quad (A-3)$$

and substitution of equations A1 and A2 into equation A3 leads to

$$P(\lambda) = \frac{1}{\pi \sigma_i \sigma_h} e^{-(\lambda - \lambda_0)^2 / \sigma_i^2 - (\lambda - \lambda_{ex})^2 / \sigma_h^2} \quad (A-4)$$

$P(\lambda)$  also has a Gaussian shape with a maximum at  $\lambda_0 + \{\sigma_i^2 / (\sigma_i^2 + \sigma_h^2)\}(\lambda_{ex} - \lambda_0)$ . The wavelength  $\lambda_{abs-max}$  where  $N(\lambda)$  is largest is thus  $\lambda_0 + \{\sigma_i^2 / (\sigma_i^2 + \sigma_h^2)\}(\lambda_{ex} - \lambda_0)$  and the maximum of the fluorescence spectrum ( $\lambda_{em}$ ) is at  $\lambda_{abs-max} + \delta$ . This leads to

$$\lambda_{em} = \lambda_0 + \delta + \frac{\sigma_i^2}{\sigma_i^2 + \sigma_h^2} (\lambda_{ex} - \lambda_0) \quad (A-5)$$

Therefore,

$$s = \frac{d(\lambda_{em})}{d(\lambda_{ex})} = \frac{\sigma_i^2}{(\sigma_i^2 + \sigma_h^2)} \quad (A-6)$$

and

$$\lambda_{em} = \lambda_0 + \delta + s(\lambda_{ex} - \lambda_0) = \lambda_{0,em} + s(\lambda_{ex} - \lambda_0) \quad (A-7)$$

Note that  $\sigma_i^2 / (\sigma_i^2 + \sigma_h^2) = \Gamma_i^2 / (\Gamma_i^2 + \Gamma_h^2) = \Gamma_i^2 \Gamma_{tot}^2$  where  $\Gamma_{tot}$  is the fwhm of the entire absorption band, caused by both homogeneous and inhomogeneous broadening.

From Eq. (A-7) the maximum  $\lambda_0$  of the total absorption band and the Stokes' shift  $\delta$  can be determined according to:

$$\lambda_0 = \lambda_{ex} - (1/s)(\lambda_{em} - \lambda_{0,em}) \quad (A-8)$$

$$\delta = \lambda_{0,em} - \lambda_0 \quad (A-9)$$

Clearly, these relations hold in the linear region of  $s$ . In the case of the red pigments in PS I, the contribution of the zero-phonon line is negligible (see Discussion and Ref. [29]) and the absorption spectrum is mainly determined by the phonon sideband. Although a Gaussian shape of this sideband is not realistic, this particular choice will not significantly influence the conclusions very much near the center of the total absorption band. For instance, a Lorentzian shape will give very similar results as long as the extreme wings of the absorption spectrum are not taken into account (calculations not shown). Finally, we note that in case the contribution of the zero-phonon line is not negligible it will lead to an increase of  $s$ , since for very small homogeneous bandwidths (like that of the zero-phonon line) the slope  $s = 1$ .

## References

- [1] Van Grondelle, R., Dekker, J.P., Gillbro, T. and Sundström, V. (1994) *Biochim. Biophys. Acta* 1187, 1–65.
- [2] Lin, S., Van Amerongen, H. and Struve, W.S. (1992) *Biochim. Biophys. Acta* 1140, 6–14.
- [3] Du, M., Xie, X., Jia, Y., Mets, L. and Fleming, G.R. (1993) *Chem. Phys. Lett.* 201, 535–542.
- [4] Werst, M., Jia, Y., Mets, L. and Fleming, G.R. (1992) *Biophys. J.* 61, 868–878.
- [5] Holzwarth, A.R., Schatz, G., Brock, H. and Bittersman, E. (1993) *Biophys. J.* 64, 1813–1826.
- [6] Trissl, H.-W. (1993) *Photosynth. Res.* 35, 247–263.
- [7] Trissl, H.-W. and Wilhelm, C. (1993) *Trends Biochem. Sci.* 18, 415–419.
- [8] Van Grondelle, R., Bergström, H., Sundström, V., Van Dorssen, R.J., Vos, M. and Hunter, C.N. (1988) in *Photosynthetic Light-Harvesting Systems* (Scheer, H. and Schneider, S., eds.), pp. 519–530, Walter de Gruyter, Berlin.
- [9] Holzwarth, A.R. (1991) in *Chlorophylls* (Scheer, H., ed.), pp. 1125–1151, CRC Press, Boca Raton, FL.
- [10] Van der Lee, J., Bald, D., Kwa, S.L.S., Van Grondelle, R., Rögner, M. and Dekker, J.P. (1993) *Photosynth. Res.* 35, 311–321.
- [11] Rögner, M., Nixon, P. and Diner, B.A. (1990) *J. Biol. Chem.* 265, 6189–6196.
- [12] Kruij, J., Boekema, E.J., Bald, D., Boonstra, A.F. and Rögner, M. (1993) *J. Biol. Chem.* 268, 23353–23360.
- [13] Kwa, S.L.S., Newell, W.R., Van Grondelle, R. and Dekker, J.P. (1992) *Biochim. Biophys. Acta* 1099, 193–202.

- [14] Kwa, S.L.S., Völker, S., Tilly, N.T., Van Grondelle, R. and Dekker, J.P. (1994) *Photochem. Photobiol.* 59, 219–228.
- [15] Boekema, E.J., Dekker, J.P., Van Heel, M., Rögner, M., Saenger, W., Witt, I. and Witt, H.T. (1987) *FEBS Lett.* 217, 283–286.
- [16] Hladík, J. and Sofrová, D. (1991) *Photosynth. Res.* 29, 171–175.
- [17] Chitnis, V.P. and Chitnis, P.R. (1993) *FEBS Lett.* 336, 330–334.
- [18] Kruip, J., Bald, D., Boekema, E.J. and Rögner, M. (1994) *Photosynth. Res.*, in press.
- [19] Wittmershaus, B.P., Woolf, V.M. and Vermaas, W.F.J. (1992) *Photosynth. Res.* 31, 75–87.
- [20] Boekema, E.J., Wynn, R.M. and Malkin, R. (1990) *Biochim. Biophys. Acta* 1017, 49–56.
- [21] Van Mourik, F., Visschers, R.W. and Van Grondelle, R. (1992) *Chem. Phys. Lett.* 193, 1–7.
- [22] Visschers, R.W., Van Mourik, F., Monshouwer, R. and Van Grondelle, R. (1993) *Biochim. Biophys. Acta* 1141, 238–244.
- [23] Kwa, S.L.S., Tilly, N.T., Eijkelhoff, C., Van Grondelle, R. and Dekker, J.P., *J. Phys. Chem.*, in press.
- [24] Völker, S. (1989) *Annu. Rev. Phys. Chem.* 40, 499–530.
- [25] Reddy, N.R.S., Lyle, P.A. and Small, G.J. (1992) *Photosynth. Res.* 31, 167–194.
- [26] Avarmaa, R.A. and Rebane, K.K. (1985) *Spectrochim. Acta* 41A, 1365–1380.
- [27] Pullerits, T., Van Mourik, F., Monshouwer, R., Visschers, R.W. and Van Grondelle, R. (1994) *J. Luminescence* 58, 168–171.
- [28] Gillie, J.K., Lyle, P.A., Small, G.J. and Golbeck, J.H. (1989) *Photosynth. Res.* 22, 233–246.
- [29] Mukerji, I. and Sauer, K. (1990) in *Current Research in Photosynthesis* (Baltscheffsky, M., ed.), Vol. II, pp. 321–324, Kluwer, Dordrecht, The Netherlands.
- [30] Jankowiak, R. and Small, G.J. (1993) in *The Photosynthetic Reaction Center* (Deisenhofer, J. and Norris, J., eds), Academic Press, New York, p. 133.